Multi-Year Planning of a Rural Microgrid Considering Storage Degradation

Article *in* Power Systems, IEEE Transactions on · March 2021

DOI: 10.1109/TPWRS.2020.3020219

CITATIONS
32

READS
251

4 authors, including:

Marina Petrelli
Politecnico di Milano
7 PUBLICATIONS **71** CITATIONS
SEE PROFILE

Davide Fioriti
Università di Pisa
82 PUBLICATIONS **785** CITATIONS
SEE PROFILE

D. Poli
Università di Pisa
124 PUBLICATIONS **1,947** CITATIONS
SEE PROFILE

Multi-year planning of a rural microgrid considering storage degradation

Marina Petrelli, *Student Member, IEEE,* Davide Fioriti, *Member, IEEE,* Alberto Berizzi, *Member, IEEE,* and Davide Poli, *Member, IEEE*

***Abstract*—Microgrids play a pivotal role in the attempts to achieve universal access to electricity; hence, their accurate planning, which also includes the evolution of the system over the project lifetime, is essential for maximizing the profitability of the investments. This paper proposes an iterative multi-year mixed-integer linear programming (MILP) optimization, in which power-dependent efficiency and capacity degradation of storage as functions of the operative strategy are considered. In this study, the computational burden of such a large problem is significantly reduced by means of an external loop that accounts for the hourly storage efficiency and residual capacity and serves to update the parameters for the MILP optimization of the following iteration. This approach is tested on a case study of a community in Soroti, in central-eastern Uganda. Comparison with the output of a one-shot MILP and with a procedure that overlooks the effects of the dispatching strategy on storage characteristics is shown, highlighting the benefits gained with the proposed algorithm in terms of both simulation time and accuracy of the design.**

***Index Terms*—Microgrid planning, MILP, rural electrification, multi-year optimization, storage degradation.**

NOMENCLATURE

Indices

h	Index of hours
y	Index of years
p	Index related to photovoltaic panels (PV)
w	Index related to wind turbines (WT)
g	Index related to diesel generators (DG)
b	Index related to batteries (BESS)
i	Set of index of components, $i \in \{g, p, w, b\}$

Parameters

M	Big constant
ε	Small constant
H	Number of hours in one year
$\overline{H}$	Project lifetime in hours
$\overline{Y}$	Project lifetime in years
Y_i^{life}	Years of life of the component
d_h	Discount factor
δ	Derating factor of salvage value of an asset
$\overline{ENS}$	Maximum allowed energy-not-served
γ_z	Forecast error of z
D_h	Load demand
$P_{h,p}^{pv}$	Available PV power generation
$P_{h,w}^{wt}$	Available WT power generation
F	Cost of fuel
H_g^{life}	Total DG working hours
A, B	Coefficients of fuel consumption curve
$\overline{P_g}$	Maximum DG working point
$\underline{P_g}$	Minimum DG working point
$\eta_{h,b}$	Working BESS efficiency
$\overline{\eta_b}$	Maximum BESS efficiency
$\overline{C_b}$	Maximum capacity of one BESS
$C_{h,b}^{res}$	Total residual capacity
DOD_b	Depth of Discharge
$\overline{PQ}_b$	Maximum power-to-energy ratio
$PQ_{h,b}$	Power-to-energy ratio
$Q_{h,b}^{thr}$	Cumulative throughput at h
$n_{h,b}^{cyc}$	Working maximum number of cycles
$\alpha_{h,b}$	Relative residual BESS capacity
$\overline{\alpha_b}$	Maximum relative BESS capacity
$\underline{\alpha_b}$	Minimum relative BESS capacity
$\beta_{h,b}$	Relative BESS efficiency
$k_{h,b}$	BESS replacement counter
ΔNPC	Loop convergence criteria on NPC variability
$\Delta\alpha$	Loop convergence criteria on $\alpha_{h,b}$ variability
$\Delta\beta$	Loop convergence criteria on $\beta_{h,b}$ variability
$\Delta\alpha_{\overline{H}}$	Loop convergence criteria on $\alpha_{h,b}$ at $\overline{H}$

Variables

NPC	Net present cost
IC_i	Initial investment cost
$O\&M_i$	Operation and maintenance cost
RC_i	Replacement cost
SV_i	Salvage value
CC_i	Capital cost of one unit
M_i	Maintenance cost of one unit
N_i	Number of units installed
D_h^u	Unmet demand
R_h	Total reserve requirement
P_h^{ren}	Renewable power injected into the system
$FC_{h,g}$	Fuel consumption
$U_{h,g}$	Number of active DG units (integer variable)
$P_{h,g}^{dg}$	Power produced by DG
$R_{h,g}^{dg}$	Reserve to be provided by DG
$Q_{h,b}$	Energy level of BESS
$P_{h,b}^{dch}$	Discharging power of BESS
$P_{h,b}^{ch}$	Charging power of BESS
$R_{h,b}^{sb}$	Reserve to be provided by BESS
$w_{h,b}^{dch}$	Binary variable equal to 1 in discharging mode

M. Petrelli and A. Berizzi are with the Department of Energy, Politecnico di Milano, Milan, 20156 Italy (e-mail: marina.petrelli@polimi.it)

D. Fioriti and D. Poli are with the Department of Energy, Systems, Territory and Construction Engineering, Università di Pisa, Pisa, 56122 Italy (e-mail: davide.fioriti@ing.unipi.it)

I. Introduction

A. Motivation

EVEN though access to electricity is increasing worldwide, there are still approximately 840 million people without any service, and most of them live in Sub-Saharan Africa [1]. The areas where this challenge has not yet been addressed are mostly rural and far from the national grid, where extension of services would be neither rapid nor cost-effective [2], [3]. Therefore, isolated systems take on great importance [4], and an effective and accurate modelling to size and operate these systems is essential to enable their dissemination in rural areas and to efficiently employ the funds allocated by private and public donors. As microgrid projects last several years, the corresponding mathematical formulation typically involves a large number of binary, integer and continuous variables; hence, simplification techniques are required, with the drawback of reducing the accuracy of simulations, especially in terms of multi-year characteristics. In particular, phenomena such as the battery capacity reduction and demand growth have a great influence on the design of the system, but they are often overlooked.

B. Microgrid sizing approaches

Many approaches have been developed for microgrid planning, and there are increasing efforts on this topic, given its urgency. In particular, the approach in [5] involves a genetic algorithm (GA) to identify a population of possible generation portfolios, on which different rule-based operating strategies are tested over one typical year, with the objective of minimizing costs, fuel use and pollutant emissions. Heuristic methods are popular when aiming to quickly find an approximate sizing, but the search space needs to be limited, often to two technologies only, to avoid incurring combinatorial explosion [6], [7]. Priority rules are identified for the employment of the available units, whose operation is analysed on the whole project lifetime in [6] and on one year in [7]. A non-dominated sorting GA (NSGA-II) is used in [8] for sizing purposes, minimizing the total cost and the load curtailment probability. Similarly, [9] implements a multi-objective NSGA-II for the design, entrusting the optimal dispatching to a 24-hour MILP. The work presented in [10] couples a GA-based sizing with an MILP optimized operation performed on 8 typical days that represent weekdays and weekends of the four seasons. A further evolutionary approach recently presented to solve the sub-problem of selecting valid-size scenarios is particle swarm optimization, also in this case followed by an MILP procedure employed to solve the downstream sub-problem of optimizing the scheduling of system components; this approach can be performed either on a 1-week interval to be averaged on the whole month, as in [11], or run on a complete year with a rolling horizon (RH) technique, as in [12]. A GA is used in [13] to identify suitable sizing scenarios, while an MILP procedure optimizes the unit commitment from weekly averaged data; then, an RH technique with a 1-hour resolution verifies the validity of the results, accordingly adjusted. Finally, the approach proposed in [14]–[17] adopts a one-shot MILP, optimizing sizing and operation all at once: the time-frame is reduced to one year represented by one typical day per month in [14] and by three typical days (week, weekend and peak) per month in [15], [16]. In addition, [17] uses the same typical days as in [15] but employs a multi-year approach in which the number of years to be optimized is flexible and adjusted to the user's knowledge of the input data and their forecast.

One of the main issues faced in these works is the trade-off between accuracy and tractability: the size of the problem is so large that, in order to guarantee the convergence of the routine, several simplifying assumptions usually need to be implemented. According to the literature review, the following three approaches are the most popular: heuristic sizing of generating and storage units coupled with rule-based dispatching of resources [5]–[8], heuristic sizing coupled with MILP-based dispatching criteria [9]–[13], and one-shot MILP performing both sizing and operation phases [14]–[17]. The first two methodologies split the formulation into two sub-problems; this usually guarantees fast computation time, with the main drawback being that the optimality of the solution cannot be assured. In contrast, optimality is not an issue in the case of the one-shot MILP. Nonetheless, the computational burden increases dramatically with the number of integer variables and time steps. For this reason, the time-frame of the simulation is usually reduced to a few representative days and strong simplifying assumptions are made to avoid non-linearities, reducing the number of non-continuous variables, and to legitimize the compression of the time interval.

C. Multi-year characteristics

The main identified research gap is the simulation and assessment of projects expected to last a considerable number of years by means of a few representative days, or at most one year, with the exception of [6], [11], [17]. This approach forces the modellers to assume that the simulated time interval is perfectly replicable along the project lifetime and to overlook any evolution over the years, thus resulting in inaccurate designs. Moreover, long-term variations are proven to have a greater impact on the cost and configuration of the system with respect to short-term variations, e.g., daily fluctuations [18]; hence, this work is focused on the former. In particular, when access to energy is provided for the first time to a rural community, it is sensible to include load growth in the model. In this regard, some methodologies have been developed, but there is no standard yet [19]. In any case, accurate data in such contexts are very difficult to collect; information are often scarce and of low quality; hence, it would be difficult to accurately tailor forecasting uncertainties, which are often more suitable for applications to industrialized countries.

Moreover, the degradation of batteries significantly affects the microgrid operational strategy during its lifetime, thus influencing optimal design of the system and vice versa. The pace at which the storage degrades depends on how it is used, and usually, replacement of the component is implemented when the capacity falls below 80% of its initial value [20], [21]. An accurate description of this phenomenon, together with other battery dynamic characteristics (e.g., variable efficiency), is pivotal for a consistent design of the microgrid.

To the authors' best knowledge, few works have managed to accurately model the battery behaviour within the scope of an MILP optimization, given the numerous non-linearities. The works [22], [23] adopt the concept of Coulomb efficiency explained in [24] to model the capacity degradation: this efficiency varies with the way the bank is operated in [22], while [23] identifies an approximation valid for any possible operating condition, and the available capacity is updated once a week. The battery life loss is a non-linear function of the state-of-charge (SOC); this curve is split into linear segments in [25] to include it into an MILP scheduling. The approach presented in [26] sets the working conditions of the storage system (C-rate, temperature) and the maximum number of cycles are consequently defined, while [27] limits the number of changes of state of the batteries to reduce degradation. Finally, a common approach is to model the capacity reduction as a function of the total throughput, regardless of how the batteries are operated [11], [17], [28]. The available storage capacity is an input parameter in most of these works, while in the case of microgrid sizing, it constitutes a variable to be optimized; this poses further linearization problems. Furthermore, none of the mentioned papers dealing with microgrid design and, consequently, with storage sizing adopts a capacity reduction model that considers the way the battery is managed. In conclusion, currently, there are no papers that address a planning problem taking into account a detailed battery model and its effects on the system operation on the entire lifespan of the project at an hourly time resolution.

D. Contributions of the work

This work aims at filling the abovementioned gap by developing a methodology able to detect the optimal sizing and operation of the plant, pursuing the least-cost objective, while capturing the complexity of such a system. The proposed methodology is based on an iterative approach with an MILP planning core that accounts for a detailed degradation of the battery efficiency and degradation while preserving convergence quality. To avoid the intractability of standard large MILP problems with many binary variables, the degradation model and the efficiency variation are taken into account by means of an iterative algorithm that updates specific constants of the MILP core. By doing so, the burden of each MILP problem is significantly reduced, but the overall approach is able to simultaneously take into account both the operational planning and the degradation of the asset performances over time, which in turn depend on the hourly scheduling. This approach makes it possible to solve this very complex problem in both an accurate and computationally efficient way. The MILP optimization is not directly used in a single shot, as in the literature, but it is embedded in an iterative scheme for the purpose of accuracy, while preserving tractability.

Therefore, the main contributions of this paper include (1) a novel iterative algorithm for multi-year planning of isolated microgrids in developing countries that (2) accurately models the variable charging-discharging efficiency of the battery and its capacity degradation as a function of the hourly power-to-energy ratio, (3) considering detailed multi-year simulations spanning the entire lifetime of the project at an hourly time resolution. The effectiveness of contribution (1) is validated by proving the infeasibility of taking into account degradation and variable efficiency of batteries in a traditional one-shot MILP. The impact of contribution (2) and (3) on the total cost of a rural microgrid in Uganda is shown, highlighting the importance of the results for real applications.

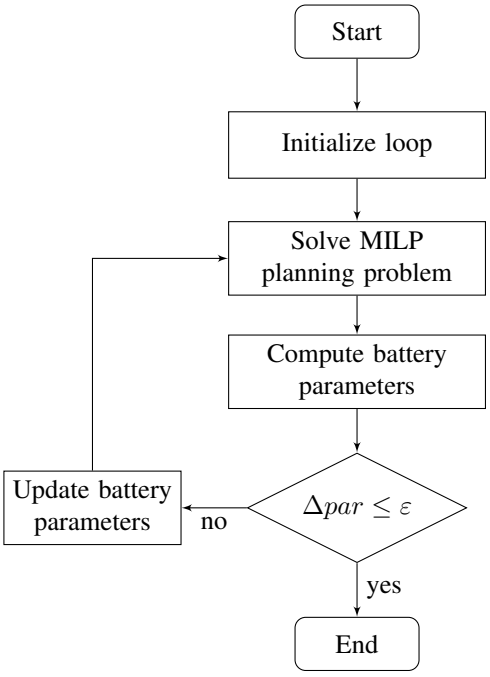

Fig. 1. The optimization algorithm.

II. Methodology

In the proposed approach, a typical planning problem is integrated with the battery power-dependent efficiency and degradation, and the long-term simulations are decomposed in the iterative algorithm depicted in Fig. 1. The main steps of the procedure are as follows:

1) Initialize the parameters describing the degradation of the battery and the power-dependent efficiency of the battery.
2) The MILP planning problem is run over the project lifetime, including the optimization of the hourly scheduling of the storage battery bank, using the most recent parameters modelling the battery. These parameters are constants for the model.
3) The parameters associated with capacity degradation and efficiency variation related to the optimized scheduling are updated.
4) If the convergence criterion on the variation of the parameters is met, the procedure stops; otherwise, the parameters are updated and a new MILP is run (go to 2).

In contrast to the standard MILP formulation that would require a large number of continuous and binary variables to be optimized inside the MILP framework, the non-linearities of the battery are modelled in the proposed method through

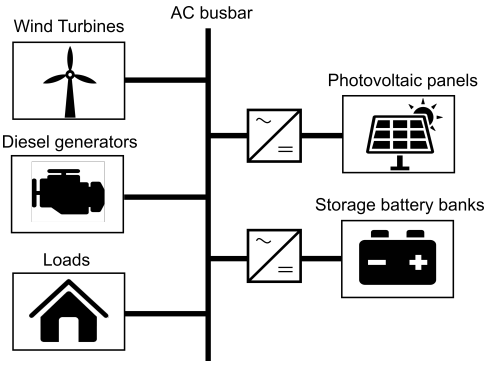

Fig. 2. Microgrid architecture

constants updated in each iteration. This reduces the computational burden of each MILP without significantly compromising the optimality of the solution. The iterative procedure runs until the variation of the parameters in two consecutive iterations falls below a threshold. The following subsections present the details of the proposed approach.

A. MILP sizing algorithm

The proposed approach is very general and can be applied to any system architecture. However, for the sake of simplicity and with no loss of generality, we describe the mathematical formulation of the method for the typical microgrid shown in Fig 2, composed by diesel generators (DG), photovoltaic panels (PV), wind turbines (WT), and battery energy storage systems (BESS). Every technology is connected to an alternating current (AC) busbar; hence, the sizing of converters (CON) is embedded into the design of the direct current (DC) units, namely, PV and BESS. An hourly time interval is considered and time-variant quantities are assumed to be constant during each interval.

The proposed model of the system aims at capturing the most significant phenomena that are incurred in the optimal design of the microgrid. Moreover, given the MILP formulation aimed at minimizing the net present cost of the system, the model automatically tends to reduce the operating costs, hence maximizing the use of renewable energy sources when available or providing time-shifting to reduce reliance on fuel-fired generators when economically profitable.

1) Objective function: The function to be minimized is the net present cost (NPC) formulated as in (1), where IC_i is the initial investment, $O\&M_i$ represents the operation and maintenance expenses, RC_i denotes the replacement cost and finally, SV_i is the salvage value.

$$NPC = \sum_i (IC_i + O\&M_i + RC_i - SV_i) \tag{1}$$

where $i \in \{g, p, w, b\}$ is the set of indexes of the available technologies, namely, DG, PV, WT and BESS, respectively; each element represents the set of available types of components for each technology.

The initial investment cost of each technology type is defined as in (2), where CC_i is the capital cost of a single unit and N_i is the number of installed units.

$$IC_i = N_i \cdot CC_i \tag{2}$$

The O&M costs are defined in (3a) for PV, WT and BESS as a fixed amount per year y, supposed to be encountered at the last hour of the year. On the other hand, the O&M costs of DG, detailed in (3b), depend upon their operation hours and on fuel expenses. M_i is the yearly O&M cost of one unit of i, $\overline{Y}$ is the project lifetime in years, H is the number of hours in one year, $\overline{H}$ is the project lifetime in hours, d_h is the discount factor in hour h, $U_{h,g}$ is the integer variable stating the number of active DG of type g in hour h, F is the cost of fuel and $FC_{h,g}$ is the hourly fuel consumption of g.

$$O\&M_{i\setminus\{g\}} = N_i \cdot M_i \cdot \sum_{y=1}^{\overline{Y}} d_{H\cdot y} \tag{3a}$$

$$O\&M_g = \sum_{h=1}^{\overline{H}} d_h \cdot (M_g \cdot U_{h,g} + F \cdot FC_{h,g}) \tag{3b}$$

Given the usual time horizon of microgrid projects, normally, the only components with a lifetime possibly shorter than the project duration are DG and BESS, and their replacement costs must be taken into account, unlike the other technologies. The life of DG is expressed in (4a) assuming H_g^{life} total working hours before replacement. The related cost is distributed along the corresponding lifetime, instead of being concentrated at the time of the actual replacement. This is a conservative approach that tends to overestimate the cost of DG, pushing towards a configuration based on renewables.

On the other hand, the presence of a replacement counter $k_{h,b}$ for BESS, increasing every time the relative residual capacity falls below the minimum threshold $\underline{\alpha_b}$, enables allocating the whole replacement cost when needed, as detailed in (4b).

$$RC_g = \frac{CC_g}{H_g^{life}} \cdot \sum_{h=1}^{\overline{H}} d_h \cdot U_{h,g} \tag{4a}$$

$$RC_b = N_b \cdot CC_b \cdot \sum_{h=1}^{\overline{H}} d_h \cdot (k_{h,b} - k_{h-1,b}) \tag{4b}$$

Finally, the salvage value of the components whose lifetime Y_i^{life} is assumed longer than the project lifetime $\overline{Y}$, namely, PV and WT, is computed in (5a). Since the DG replacement cost is addressed as a distributed cost, there is no need to consider its salvage value, which is instead evaluated for BESS in (5b) based on the residual capacity available. $\alpha_{h,b}$ is the per-unit BESS residual capacity, bounded in between a maximum ($\overline{\alpha_b}$) and a minimum ($\underline{\alpha_b}$) threshold. Factor δ serves the aim of derating the value of an asset when sold after usage.

$$SV_{i\setminus\{g,b\}} = \delta \cdot d_{\overline{H}} \cdot N_i \cdot CC_i \frac{Y_i^{life} - \overline{Y}}{Y_i^{life}} \tag{5a}$$

$$SV_b = \delta \cdot d_{\overline{H}} \cdot N_b \cdot CC_b \cdot \frac{\alpha_{\overline{H},b} - \underline{\alpha_b}}{\overline{\alpha_b} - \underline{\alpha_b}} \tag{5b}$$

2) Constraints: The power balance constraint at the AC busbar is reported in (6), where $P_{h,b}^{dch}$ is the discharging power from BESS of type b, $\overline{\eta_b}$ is the maximum BESS efficiency of b, $\beta_{h,b}$ is the per-unit BESS efficiency of hour h, $P_{h,b}^{ch}$ is the BESS charging power of BESS of type b, P_h^{ren} is the renewable power injected into the system, $P_{h,g}^{dg}$ is the power produced by the DG units of type g, D_h^u is the unmet demand and D_h is the demand.

$$\sum_b \left(P_{h,b}^{dch} \cdot \overline{\eta_b} \cdot \beta_{h,b} - \frac{P_{h,b}^{ch}}{\overline{\eta_b} \cdot \beta_{h,b}} \right) + \\ + P_h^{ren} + \sum_g P_{h,g}^{dg} + D_h^u = D_h \tag{6}$$

To avoid the oversizing of the system, load shedding is typically admitted in these contexts. In particular, in the proposed formulation, the constraint is enforced to be below a given threshold of the yearly demand (see (7)), so that significant mismatches of unmet demand along the project lifetime are avoided. In the literature, sometimes the same problem is modelled by using economic penalties in the objective function for every unit of energy-not-served (ENS) [29], while other studies have proposed the formulation by hard constraints [6], [30], as developed in this work. Both models involve considerations on continuity of supply and provide similar results, but the former is computationally more demanding as highlighted in [29]. Moreover, given the scope of application of the model, it may be difficult to identify the numerical value to be used in such contexts. Last, public call for tender may often have requirements in terms of a cap on ENS rather than estimating its equivalent economic cost. Therefore, the second approach is selected: load curtailment is admitted and capped in (7) through the $\overline{ENS}$ factor.

$$\sum_{h=1}^{\overline{H}} D_{(y-1)\cdot\overline{H}+h}^u \leq \sum_{h=1}^{\overline{H}} D_{(y-1)\cdot\overline{H}+h} \cdot \overline{ENS} \tag{7}$$

The renewable production injected into the system computed in (8) is at most equal to its availability, where $P_{h,p}^{pv}$ is the generation available from the PV generator of type p, and $P_{h,w}^{wt}$ is the generation available from the WT generator of type w.

$$P_h^{ren} \leq \sum_p N_p \cdot P_{h,p}^{pv} + \sum_w N_w \cdot P_{h,w}^{wt} \tag{8}$$

The next block of constraints is devoted to defining the behaviour of DG. In particular, (9a) describes a linear fuel consumption curve according to coefficients A and B, suitable for small size DG; (9b) and (9c) limit the working area of the units within $\overline{P_g}$ and $\underline{P_g}$ and consider the reserve $R_{h,g}^{dg}$ to be provided; and (9d) limits the total number of active generators.

$$FC_{h,g} = A \cdot U_{h,g} + B \cdot P_{h,g}^{dg} \tag{9a}$$

$$P_{h,g}^{dg} + R_{h,g}^{dg} \leq \overline{P_g} \cdot U_{h,g} \tag{9b}$$

$$P_{h,g}^{dg} \geq \underline{P_g} \cdot U_{h,g} \tag{9c}$$

$$U_{h,g} \leq N_g \tag{9d}$$

The behaviour of BESS is ruled by (10a)-(10g), where (10a) defines the energy level $Q_{h,b}$, limited by (10b) and (10c); the discharging and charging power are capped in (10d) and (10e) by the maximum power-to-energy ratio $\overline{PQ}_b$; and (10f) and (10g) aim at avoiding that the batteries discharge and charge during the same time interval. Δh is the selected time interval, $\overline{C_b}$ is the maximum capacity of one unit of b, DOD_b is the depth of discharge, $R_{h,b}^{sb}$ is the reserve to be provided by BESS of type b, $w_{h,b}^{dch}$ is a binary variable equal to 1 in the discharging mode and 0 in the charging mode, and M is a large constant.

$$Q_{h,b} = Q_{h-1,b} + (P_{h,b}^{ch} - P_{h,b}^{dch}) \cdot \Delta h \tag{10a}$$

$$Q_{h,b} \geq N_b \cdot \overline{C}_b \cdot (1 - DOD_b) + R_{h,b}^{sb} \tag{10b}$$

$$Q_{h,b} \leq \alpha_{h,b} \cdot N_b \cdot \overline{C_b} \tag{10c}$$

$$P_{h,b}^{dch} \leq N_b \cdot \overline{C_b} \cdot \overline{PQ}_b \tag{10d}$$

$$P_{h,b}^{ch} \leq N_b \cdot \overline{C_b} \cdot \overline{PQ}_b \tag{10e}$$

$$P_{h,b}^{dch} \leq w_{h,b}^{dch} \cdot M \tag{10f}$$

$$P_{h,b}^{ch} \leq (1 - w_{h,b}^{dch}) \cdot M \tag{10g}$$

To account for the unpredictability related to real-time dispatching of the system, a reserve requirement R_h to be provided by DG and BESS is established in (11), proportional to the unpredictability of load (γ_d) and availability of renewables (γ_{pv} and γ_{wt}). The literature is rich with different approaches that differ in terms of data and computational requirements; however, the use of reserves is generally computationally efficient [7], [10], and the authors regarded the approach as a good compromise between tractability and representation of the problem, especially with respect to stochastic [6], [29] or robust [31] optimization. In stochastic optimization, uncertainties are often modelled by means of scenarios, which proportionally increase the size of the problem with often more than a linear increase of computational requirements; that is the reason why often representative days are used and/or no battery dynamics are considered in the literature. Moreover, the formulation of scenarios and of their probability distribution requires an amount of data that is hardly available for developing countries. On the other hand, robust optimization provides a configuration able to completely fulfil the demand for any realization of the inputs [31]. The method is computationally efficient, but it tends to oversize the generating units, leading to a higher overall cost [32], [33]. Hence, it is likewise unsuitable for our purpose because affordability is often a priority over reliability of service in cases of first access provided to rural communities. For these reasons, the approach involving reserve requirements is preferred.

$$R_h = \gamma_d \cdot D_h + \gamma_{pv} \cdot \sum_p N_p \cdot P_{h,p}^{pv} + \\ + \gamma_{wt} \cdot \sum_w N_w \cdot P_{h,w}^{wt} \tag{11a}$$

$$R_h \leq \sum_g R_{h,g}^{dg} + \sum_b R_{h,b}^{sb} \cdot \overline{\eta_b} \cdot \beta_{h,b} \tag{11b}$$

B. Update of MILP parameters

As shown in the previous subsection, the dynamic behaviour of BESS in terms of capacity degradation and variable efficiency is accounted for in the MILP optimization by means

of the parameters $\alpha_{h,b}$ and $\beta_{h,b}$, respectively. The former quantifies the relative residual capacity at hour h, depending on the total throughput $Q^{thr}_{h,b}$ and on the working power-to-energy ratio $PQ_{h,b}$. The latter indicates the relative charging or discharging efficiency, and it varies according to the working $PQ_{h,b}$, which is computed as in (12) after each MILP problem is solved:

$$PQ_{h,b} = \frac{P^{ch}_{h,b} + P^{dch}_{h,b}}{N_b \cdot \overline{C_b}} \tag{12}$$

The value of $PQ_{h,b}$ has to comply with the maximum power rate of the component ($PQ_{h,b} \in [0; \overline{PQ_b}]$), and it is discretized in subintervals, each characterized by a constant maximum number of cycles $n^{cyc}_{h,b}$ (i.e., the BESS cycle lifetime if always operated at that $PQ_{h,b}$) and charging and discharging efficiencies $\eta_{h,b}$. At each hour h, $n^{cyc}_{h,b}$ and $\eta_{h,b}$ are assigned according to the relevant interval of $PQ_{h,b}$. The computation of the parameter $\beta_{h,b}$ in (13) is now straightforward.

$$\beta_{h,b} = \frac{\eta_{h,b}}{\overline{\eta_b}} \tag{13}$$

To calculate $\alpha_{h,b}$, first, the total throughput is computed according to (14).

$$Q^{thr}_{h,b} = Q^{thr}_{h-1,b} + (P^{ch}_{h,b} + P^{dch}_{h,b}) \cdot \Delta h \tag{14}$$

The BESS residual capacity $C^{res}_{h,b}$ is modelled as a sawtooth function: in (15a), it degrades linearly as $Q^{thr}_{h,b}$ increases, with a growing slope for increasing $PQ_{h,b}$, i.e., decreasing $n^{cyc}_{h,b}$, and no replacement is needed; conversely, in (15b), it returns to its initial value when $\alpha_{h,b}$ falls below $\underline{\alpha_b}$, i.e., a replacement is put in place.

$$\text{if } \alpha_{h-1,b} \geq \underline{\alpha_b} \begin{cases} C^{res}_{h,b} = C^{res}_{h-1,b} - \dfrac{1-\underline{\alpha_b}}{2 \cdot n^{cyc}_{h,b} \cdot DOD_b} \cdot \\ \qquad \cdot (Q^{thr}_{h,b} - Q^{thr}_{h-1,b}) \\ k_{h,b} = k_{h-1,b} \end{cases} \tag{15a}$$

$$\text{if } \alpha_{h-1,b} < \underline{\alpha_b} \begin{cases} C^{res}_{h,b} = N_b \cdot \overline{C_b} \\ k_{h,b} = k_{h-1,b} + 1 \end{cases} \tag{15b}$$

Finally, the parameter $\alpha_{h,b}$ is computed as detailed in (16).

$$\alpha_{h,b} = \frac{C^{res}_{h,b}}{N_b \cdot \overline{C_b}} \tag{16}$$

C. Convergence criteria

Convergence of the algorithm is achieved when the following criteria are met. First, the NPC is compared with the value obtained in the previous iteration NPC^*, and the relative change ΔNPC, calculated as in (17), shall fall below a given threshold.

$$\Delta NPC = \frac{|NPC - NPC^*|}{NPC} \tag{17}$$

Furthermore, in order to stress the convergence of the algorithm and improve the NPC, we also introduced convergence criteria on the degrading effects of the assets, modelled by the parameters $\alpha_{h,b}$ and $\beta_{h,b}$. In two consecutive MILP optimizations, only the degradation parameters ($\alpha_{h,b}$ and $\beta_{h,b}$) are modified; therefore, when limited changes occur on these parameters, limited differences in the optimal design of the master MILP problem are expected; hence, this strengthened convergence criterion is expected to provide more reliable solutions.

The relative change in the parameters $\alpha_{h,b}$ and $\beta_{h,b}$ is detailed in (18a)-(18c).

$$\Delta\alpha = \frac{\sum_{h,b} \left|\alpha_{h,b} - \alpha^*_{h,b}\right|}{\sum_{h,b} \alpha_{h,b}} \tag{18a}$$

$$\Delta\beta = \frac{\sum_{h,b} \left|\beta_{h,b} - \beta^*_{h,b}\right|}{\sum_{h,b} \beta_{h,b}} \tag{18b}$$

$$\Delta\alpha_{\overline{H}} = \frac{\left|\alpha_{\overline{H},b} - \alpha^*_{\overline{H},b}\right|}{\alpha_{\overline{H},b}} \tag{18c}$$

$\Delta\alpha$ and $\Delta\beta$ focus on the average absolute variation of the parameters, while $\Delta\alpha_{\overline{H}}$ evaluates the relative change in the battery energy degradation occurring at the end of the project. The rationale behind using the average criterion of $\Delta\alpha$ and $\Delta\beta$ is justified by the fact that when a relative mipgap [34] higher than zero takes place, in two consecutive iterations, the algorithm may replace the battery in the same day, but not exactly in the same hour, which may lead $\Delta\alpha$ up to $\underline{\alpha_b}$ in the replacement hour, preventing the convergence of the procedure but with no significant effect in terms of optimality of the solution. By using the average absolute criterion, the above numerical instability is mitigated. Nevertheless, (18c) guarantees congruity in terms of residual capacity at the end of the project and, consequently, of time of replacement. In fact, even if the time of replacement slightly changes at convergence, the variation in the residual capacity would be negligible; therefore, equation (18c) increases the stability of the approach with respect to convergence criteria on the maximum difference at any hour.

III. Case study

A. Location and input data

The methodology proposed in the previous section has been tested on a rural community based in Soroti, in central-east of Uganda (1.72N 33.6E). Data on local availability of solar and wind power production have been acquired by means of the Renewable.ninja web platform [35], [36]. To represent the multi-year behaviour of the proposed community and its hourly uncertainties, the load profile, shown in Fig. 3, has been estimated by accounting for the dynamics of the social behaviour of the community over the considered time horizon (10 years) based on the results of the study on social-dynamics developed in [37]. The methodology described in [38] has been developed with different input data for each year, in order to reproduce the relative load growth estimated in [37], due to the growth in the users and the higher penetration of appliances; the latter is estimated by using the income percentiles for the proposed community [39]. Users have been grouped in 17 different classes (6 residential, 11 business activities and local services), whose size and number of appliances per customer grow over time; in particular, we assumed the demand estimated in [38] refers to the last year

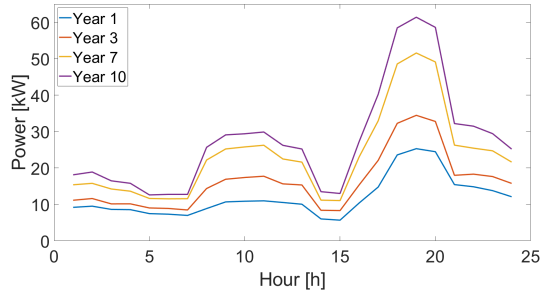

(a)

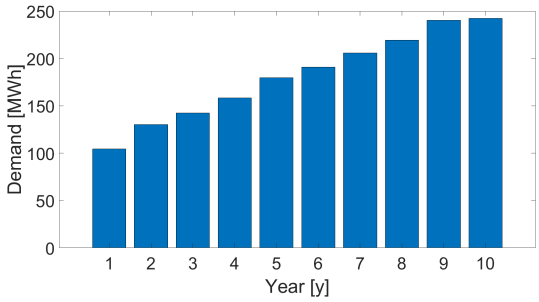

(b)

Fig. 3. Estimated load profiles (a) and total yearly demand (b)

TABLE I
COMPONENTS COSTS AND LIFETIMES [7], [8], [11], [12]

	Unit size	CC(x)	M(x)	Lifetime
PV	1 kW	1.1 k€	10 €/y	20 y
WT	10 kW	27 k€	810 €/y	20 y
DG	16 kW	11 k€	0.208 €/h	15,000 h
BESS	1 kWh	0.4 k€	10 €/y	15 y
CON	1 kW	0.3 k€	0 €	20 y

of the project, and we went back in estimating the profiles of the previous years by reproducing the growth trends analysed in [37]. By using the methodology described in [38], 20 load profiles were calculated for every year of the simulation to assess the hourly uncertainties of the typical profile, which was calculated by averaging the 20 profiles. A Monte Carlo technique was used to draw the daily profiles of the entire year: a Gaussian noise was added to the daily average load, whose standard deviation equals the one calculated for the 20 different profiles of the corresponding year. The granularity of both renewable generation and demand profiles is 1 hour.

The capital and maintenance costs of the different units are shown in Table I together with their maximum lifetime. A DG fuel cost of 0.75 €/l is considered. Table II shows the features of the selected Li-ion battery model. The parameters in Tables I and II were derived from a literature review and the authors' experience. Realistic ranges of the power-to-energy ratio dependent characteristics were derived from the literature [40]–[42] and are provided in Table III.

TABLE II
BESS SPECIFICATIONS [6], [7], [42]

Nominal capacity of one BESS unit $\overline{C}_b$	1	kWh
Maximum power-to-energy ratio $\overline{PQ}_b$	1	kW/kWh
Depth of Discharge DOD_b	90	%
Initial State-of-Charge SOC_b^{init}	100	%
Minimum residual capacity before replacement $\underline{\alpha}_b$	80	%

TABLE III
BESS CHARACTERISTICS DEPENDING ON $PQ_{h,b}$ [40]–[42]

	$PQ_{h,b} \leq 0.2$	$0.2 < PQ_{h,b} \leq 0.6$	$PQ_{h,b} > 0.6$
$\eta_{h,b}$	99%	98%	95%
$n_{h,b}^{cyc}$	3500	3200	3000

B. Simulation parameters

When dealing with electrification projects in developing countries, it is advisable to consider a limited project duration with respect to the expected lifetime of the components to limit risks, given that many changes can arise in a newly electrified community. For this reason, a project lifetime of 10 years is considered. Moreover, as in these contexts, a limited loss of continuity of service comes with almost null social cost; a yearly loss of load of 5% is admitted [6]. The discount factor d_h is computed based on an 8% nominal interest rate and a 2% expected inflation rate.

C. Test procedure

To prove the effectiveness of the method, the following models have been developed, tested and compared:

1) Iterative Multi-Year (IMY): the proposed iterative procedure, depicted in Fig. 1, accounting for battery degradation and variable efficiency in a multi-year environment at an hourly time resolution.
2) One-Shot Multi-Year (OSMY): a standard literature-based methodology equivalent to IMY but developed in a full MILP environment with no iterative algorithm.
3) IMY without battery details (IMYwoB): the proposed iterative method (IMY) without accounting for the battery degradation and variable efficiency. This simulation aims at highlighting the benefits of considering the battery degradation since the planning phase.
4) IMY and OSMY with representative days (IMYrd/OSMYrd): in order to facilitate OSMYrd to converge and to be able to validate the results of IMY and OSMY, both IMY and OSMY are developed using 20 representative days (1 per season, with each year characterized by a rainy and a dry season in the area of interest).
5) Sensitivity on battery lifetime (IMY±25%): in order to evaluate the effects of the battery lifetime on the optimal design, a sensitivity analysis is performed by increasing and decreasing the lifetime of the battery ($n_{h,b}^{cyc}$) by $\pm 25\%$.

The convergence of the MILP optimization has been ruled by a maximum gap [34] of 3%, the tolerances of the external

loop related to BESS behaviour (see (18)) have been all set to 1%, and the convergence criterion on the stability of the objective function (see (17)) has been fixed at 3%, coherently with the mipgap. A limit of 5 days has been set for the duration of the simulations. These values have been tailored according to the literature and experience of the authors. It is worth noticing that information regarding the optimality gap is rarely disclosed, even if it plays a pivotal role in the tractability/accuracy trade-off. The optimal microgrid sizing is found in [29] and [43] by setting a 5% mipgap for a similar formulation; both the algorithms are run on one year with hourly time steps but no long-term phenomenon is taken into account. Nevertheless, the time employed by the two algorithms to converge is in the range of a few hours, comparable with the computational burden of the work presented here, which is characterized by a much larger size (1.66 million constraints and 1.31 million variables) and a lower mipgap.

The algorithm has been modelled in GAMS 24.0.2 and solved with CPLEX. The simulations have been run on a 6-core 3.20 GHz Intel Core i7 computer with 16 GB RAM.

IV. Results and discussion

The main results of all the proposed tests are discussed in the following sections. The main outcomes in terms of computational burden, sizing, objective function, cost components, BESS replacement year Y_b^{repl} and residual capacity at the end of the project $\alpha_{\overline{H},b}$ have been summarized in Table IV.

A. The advantages of the proposed approach

The first noticeable result is that OSMY has not converged within the time limit of 5 days: CPLEX was still branching to find a first integer-feasible solution for the proposed problem; hence, no MIP gap was available. This underlines the complexity for standard MILP formulations to handle the proposed planning problem, while the IMY approach discussed in this activity successfully converged in 5.5 hours, reaching the target tolerances in 3 iterations. Therefore, the gain in terms of tractability of the algorithm is impressive, and this confirms that the proposed iterative algorithm can easily contend with multi-year planning problems with battery degradation and variable efficiency with low requirements in contrast to other standard techniques such as OSMY. Finally, the optimization IMYwoB, which neglects battery degradation and variable efficiency ($\alpha_{h,b} = 1$ and $\beta_{h,b} = 1$ in every time step), converged in 3.5 hours, which strengthens the robustness of IMY in reducing the requirements of one-shot methodologies.

Given that our results are characterized by a 3% mipgap, the comparison underlines the computational efficiency of the proposed method with respect to the literature [29], [43].

B. Impact of BESS degradation on planning and operation

To evaluate the effects of the battery degradation and variable efficiency, the proposed methodology (IMY) is compared to IMYwoB, which neglects the above. The results show that NPC with IMY is approximately 17% higher than IMYwoB, which suggests that neglecting such phenomena may lead to a suboptimal design of the system. As a matter of fact, in IMYwoB, the load is largely powered by renewable sources, especially during the first four years, due to a larger PV plant supported by storage; as the load grows, the diesel production commences, but its share never exceeds 31% of the total demand (see Fig. 4a). With respect to IMY, this configuration comes with higher investment costs but limited O&M costs; moreover, as no battery degradation is accounted for, the components have high residual value at the end of the project and the replacement costs are only related to the DG working hours, as described by (4a). That suggests, however, that in the real operation, the battery degradation would reduce the capability of the system to defer to the renewable production; hence, the reliance on the fuel generator or higher ENS are likely to occur.

By considering battery degradation and variable efficiency since the planning phase as in IMY, the result will be tailored to the actual system's behaviour; in fact, the optimizer tends to employ more DG and to leave a less prominent role to PV and BESS, whose size is reduced by 13% and 20%, respectively, and which are able to cover alone only the load of year 1 (see Fig. 4b). In the last year of the project, PV panels are only providing energy to 54% of the demand, compared to the 64% of IMYwoB. Now, the NPC is 17% higher, characterized by a more consistent portion of O&M costs, approximately 35% higher than the O&M in IMYwoB and mainly related to fuel consumption, while the initial investment is reduced by 15%.

The results show that the model tends to avoid the replacement of the battery: the net capacity level (83%) at the end of the optimization period is very close to the replacement threshold (80%), as shown in Fig. 5. Hence, the accurate modelling of the storage behaviour has a strong impact on the optimization results, as the system gradually ends up working with a way smaller BESS availability.

The trend of fuel consumption along the years in the two tests is compared in Fig. 6: in both cases, the growing utilization of diesel generators follows the increase in the demand, but the degradation of BESS in IMY makes the use of DG necessary two years in advance. Furthermore, the use of discounted cash flows for NPC evaluation induces the optimizer to favour outflows in the late years, leaning towards a more frequent utilization of diesel units, rather than oversizing the renewable plant and the storage capacity, which explains the delay in the employment of DG in both cases. The local wind availability is not enough to induce the optimizer to consider the installation of wind turbines, either in IMY or IMYwoB.

C. Stability and computational efficiency of the results

To highlight the good convergence performances of the proposed algorithm, IMY has been run for 5 additional iterations after the convergence criteria were met, and the corresponding behaviour of the convergence parameters and of the objective function are shown in Fig. 7. It is worth noticing that the value of the objective function is stable after 3 iterations as well as parameters $\alpha_{h,b}$ and $\beta_{h,b}$. This is the reason why the corresponding relative changes, namely, ΔNPC, $\Delta\alpha$ and

TABLE IV
OPTIMIZATION OUTPUTS

	Time [h]	NPC [k€]	IC [k€]	O&M [k€]	RC [k€]	SV [k€]	PV [kW]	WT [kW]	DG [kW]	BESS [kWh]	Y_b^{repl} [y]	$\alpha_{\overline{H},b}$ [%]
IMY	5.5	316	228	111	17	40	86	/	16	215	/	83
IMYwoB	3.5	271	269	82	13	93	98	/	16	268	/	100
OSMY*	>120	/	/	/	/	/	/	/	/	/	/	/
IMYrd	$8.3\ 10^{-4}$	301	216	104	16	35	80	/	16	206	/	82
OSMYrd	97.2	297	222	98	14	37	81	/	16	218	/	82
IMY-25%	11.4	335	220	115	66	66	83	/	16	205	9	97
IMY+25%	4.93	307	222	113	17	45	84	/	16	207	/	86

* No feasible solution reached in the given time limit: CPLEX was still branching to find a first feasible integer solution.

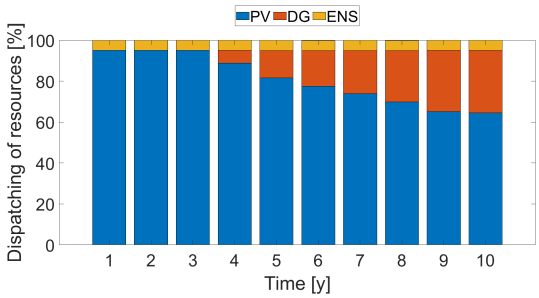

(a)

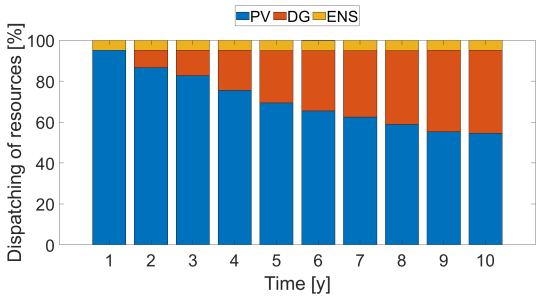

(b)

Fig. 4. Dispatching of resources in IMYwoB (a) and IMY (b)

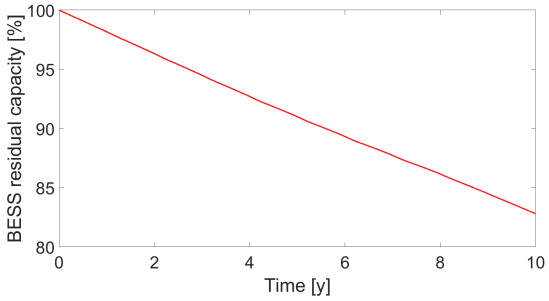

Fig. 5. Storage capacity degradation in IMY

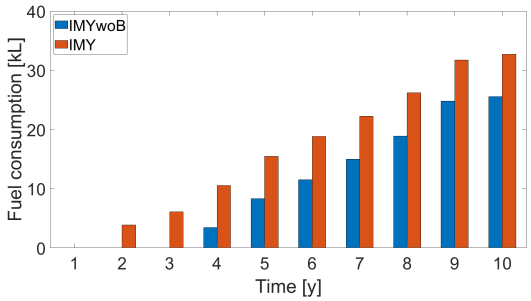

Fig. 6. Fuel consumption in IMYwoB and IMY

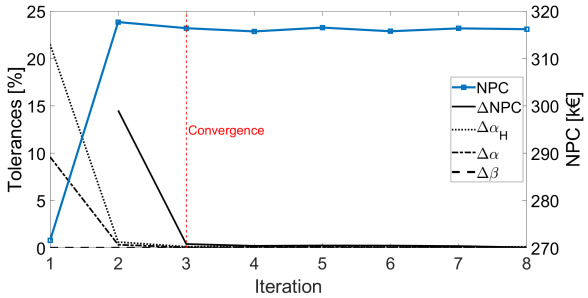

Fig. 7. Evolution along the procedure's iterations of the convergence criteria and of the objective function

$\Delta\alpha_{\overline{H}}$, fall below the convergence threshold in few iterations and the procedure stops. The large NPC error of the first iteration occurs because the first MILP is initialized with no battery degradation; hence, the sizing corresponds to the output of IMYwoB. Starting from the second iteration, the effects of degradation and variable efficiency commence and PV and BESS are downsized, and the reliance on diesel increases. Along the iterative procedure, the available DG power remains constant and the number of PV and BESS units installed undergoes slight oscillations. The convergence is reached not only when the final sizing is attained but also when the algorithm selects the optimal operation of the installed components. The proposed convergence criteria meet both: ΔNPC accounts for the total project costs, accounting for both the investment and operating costs, while $\Delta\alpha$ and $\Delta\beta$ focus on the operating effects. In the proposed simulations, battery degradation has a more significant impact than variable efficiency. $\Delta\alpha$ parameters experience a larger dynamic than $\Delta\beta$, as shown in Fig. 7, which can be explained by the fact that the hourly power-to-energy ratio $PQ_{h,b}$ usually stays below the 0.2 threshold since it is profitable to install a large battery and perform time-shifting of the energy produced by the PV source.

D. Validation using typical days

The results reported in Table IV highlight that when representative days are used, the proposed methodology (IMYrd) and the one-shot one (OSMYrd) converge towards similar designs and values of the objective function; small differences are justified by the 3% mipgap. It is worth noticing that the errors in terms of NPC are approximately 1% and the difference in terms of installed components is very limited. Despite the low number of representative days, the computational requirement of OSMYrd is still very high (more than 4 days), while IMYrd requires a few seconds to converge, which emphasizes the advantages and benefits of the proposed approach, as already discussed. Furthermore, the results with IMYrd and OSMYrd are also similar to the values of IMY and OSMY, which strengthens the quality of the approach, but IMY is still preferable given its faster convergence and its higher capability of describing the real dynamics of the system; in fact, NPC with IMY is 6.4% higher than that with OSMYrd. However, methodologies with representative days, such as IMYrd, can be useful tools for preliminary designs given their low computational requirements.

E. Sensitivity analysis on BESS degradation parameters

Since battery lifetime is a critical element in planning phases, subject to significant uncertainties, a sensitivity analysis on the lifetime of the BESS has been performed, and the results are shown in Table IV. As expected, the higher the battery lifetime is, the lower the total NPC, as in the test IMY+25%, corresponding to a lifetime 25% higher than IMY, the NPC is 2.8% lower than IMY, while it increases by 6% in IMY-25%. The higher costs of IMY-25% are related to the need of performing a BESS replacement at year 9 and to a 7% higher utilization of DG. These results suggest how the cost of using batteries with a lower lifetime is higher that the benefit of increasing the lifetime by the same amount, and it underlines the great importance and urgency of developing a planning methodology able to cope with battery degradation in real applications. The above achievement is also enforced by the low computational requirements of the approaches, always below 12 hours, as shown in Table IV.

V. Conclusion

The novel procedure proposed in this study, based on an iterative approach with an internal MILP core, successfully addresses the planning of a rural off-grid microgrid with a detailed multi-year horizon at an hourly time resolution. This approach enables analysing the dynamics of load growth and storage degradation with its power-dependent efficiency throughout the entire project lifetime, with significant benefits for developers.

The proposed approach has been compared to traditional methods, validation tests have been performed by using representative days, and a sensitivity analysis over the battery lifetime has also been discussed. The results highlight significant improvements with respect to the equivalent literature-based one-shot MILP. The great advantage of the new method derives from outsourcing the calculations related to battery behaviour to an external loop, which reduces the computational requirements without affecting the quality of the results, as discussed in the proposed validation. Representative days can be used in preliminary analyses for rough evaluations, but the full methodology proposed in this paper is recommended for the advanced design, given the higher accuracy of the results. Dedicated simulations highlight that neglecting the effects of battery degradation and power-dependent efficiency can lead to underestimating the cost of the system even by 17%, which may lead to sub-optimal allocation of resources and, most likely, energy shortages and financial issues. Similarly, the sensitivity over the battery lifetime has proven the battery to be a critical component, which can be accurately taken into account by our approach.

This methodology is expected to significantly advance the current state of the art in planning algorithms including the non-linear constraints of the dynamics of the battery. In particular, it can be implemented in real case studies and sizing tools so that developers can benefit by more accurate simulations of the system behaviour, thus having a more appropriate understanding of the financial and technical requirements of their investments. The approach can be easily adapted to different system configurations and typologies, eventually including modular upgrades of the system during the project lifetime or relaxing the assumption of perfect knowledge of the demand and renewable availability.

References

[1] IEA, International Renewable Energy Agency, United Nations Statistics Division, The World Bank, and World Health Organization, "The Energy Progress Report," p. 176, 2019.

[2] J. P. Murenzi and T. S. Ustun, "The case for microgrids in electrifying Sub-Saharan Africa," *IREC2015 The Sixth International Renewable Energy Congress*, pp. 1–6, 2015.

[3] A. H. Hubble and T. S. Ustun, "Scaling renewable energy based microgrids in underserved communities: Latin America, South Asia, and Sub-Saharan Africa," *IEEE PES PowerAfrica Conference, PowerAfrica 2016*, pp. 134–138, 2016.

[4] Energy Sector Management Assistance Program, "Mini Grids for Half a Billion People: Market Outlook and Handbook for Decision Makers. ESMAP Technical Report," 2019.

[5] B. Zhao, X. Zhang, P. Li, K. Wang, M. Xue, and C. Wang, "Optimal sizing, operating strategy and operational experience of a stand-alone microgrid on Dongfushan Island," *Applied Energy*, vol. 113, pp. 1656–1666, 2014.

[6] C. Brivio, M. Moncecchi, S. Mandelli, and M. Merlo, "A novel software package for the robust design of off-grid power systems," *Journal of Cleaner Production*, vol. 166, pp. 668–679, 2017.

[7] L. Moretti, M. Astolfi, C. Vergara, E. Macchi, J. I. Pérez-Arriaga, and G. Manzolini, "A design and dispatch optimization algorithm based on mixed integer linear programming for rural electrification," *Applied Energy*, vol. 233-234, pp. 1104–1121, 2019.

[8] A. Kamjoo, A. Maheri, A. M. Dizqah, and G. A. Putrus, "Multi-objective design under uncertainties of hybrid renewable energy system using NSGA-II and chance constrained programming," *International Journal of Electrical Power and Energy Systems*, vol. 74, pp. 187–194, 2016.

[9] L. Guo, W. Liu, J. Cai, B. Hong, and C. Wang, "A two-stage optimal planning and design method for combined cooling, heat and power microgrid system," *Energy Conversion and Management*, vol. 74, pp. 433–445, 2013.

[10] J. Zhang, K. J. Li, M. Wang, W. J. Lee, and H. Gao, "A bi-level program for the planning of an islanded microgrid including CAES," *IEEE Industry Application Society - 51st Annual Meeting, IAS 2015, Conference Record*, pp. 1–8, 2015.

[11] D. R. Prathapaneni and K. P. Detroja, "An integrated framework for optimal planning and operation schedule of microgrid under uncertainty," *Sustainable Energy, Grids and Networks*, vol. 19, p. 100232, 2019.

[12] D. Fioriti, R. Giglioli, D. Poli, G. Lutzemberger, A. Micangeli, R. Del Citto, I. Perez-Arriaga, and P. Duenas-Martinez, "Stochastic sizing of isolated rural mini-grids, including effects of fuel procurement and operational strategies," *Electric Power Systems Research*, vol. 160, pp. 419–428, 2018.

[13] B. Li, R. Roche, and A. Miraoui, "Microgrid sizing with combined evolutionary algorithm and MILP unit commitment," *Applied Energy*, vol. 188, pp. 547–562, 2017.

[14] N. E. Koltsaklis, M. Giannakakis, and M. C. Georgiadis, "Optimal energy planning and scheduling of microgrids," *Chemical Engineering Research and Design*, vol. 131, pp. 318–332, 2018.

[15] S. Mashayekh, M. Stadler, G. Cardoso, and M. Heleno, "A mixed integer linear programming approach for optimal DER portfolio, sizing, and placement in multi-energy microgrids," *Applied Energy*, vol. 187, pp. 154–168, 2017.

[16] S. Mashayekh, M. Stadler, G. Cardoso, M. Heleno, S. C. Madathil, H. Nagarajan, R. Bent, M. Mueller-Stoffels, X. Lu, and J. Wang, "Security-Constrained Design of Isolated Multi-Energy Microgrids," *IEEE Transactions on Power Systems*, vol. 33, no. 3, pp. 2452–2462, 2018.

[17] Z. K. Pecenak, M. Stadler, and K. Fahy, "Efficient multi-year economic energy planning in microgrids," *Applied Energy*, vol. 255, no. April 2019, p. 113771, 2019.

[18] F. Riva, F. Gardumi, A. Tognollo, and E. Colombo, "Soft-linking energy demand and optimisation models for local long-term electricity planning: An application to rural India," *Energy*, vol. 166, pp. 32–46, 2019.

[19] F. Riva, A. Tognollo, F. Gardumi, and E. Colombo, "Long-term energy planning and demand forecast in remote areas of developing countries: Classification of case studies and insights from a modelling perspective," *Energy Strategy Reviews*, vol. 20, pp. 71–89, 2018.

[20] H. Bindner, T. Cronin, P. Lundsager, J. F. Manwell, U. Abdulwahid, and I. Baring-gould, *Lifetime Modelling of Lead Acid Batteries*, 2005, vol. 1515, no. April.

[21] N. Diorio, A. Dobos, S. Janzou, A. Nelson, and B. Lundstrom, "Technoeconomic Modeling of Battery Energy Storage in SAM," *NREL Technical Report NREL/TP-6A20-64641*, no. September, 2015.

[22] A. Perez, R. Moreno, R. Moreira, M. Orchard, and G. Strbac, "Effect of Battery Degradation on Multi-Service Portfolios of Energy Storage," *IEEE Transactions on Sustainable Energy*, vol. 7, no. 4, pp. 1718–1729, 2016.

[23] D. Jimenez, D. Ortiz-Villalba, A. Perez, and M. E. Orchard, "Lithium-ion battery degradation assessment in microgrids," *2018 IEEE International Autumn Meeting on Power, Electronics and Computing, ROPEC 2018*, 2019.

[24] A. Pérez, V. Quintero, H. Rozas, F. Jaramillo, R. Moreno, and M. Orchard, "Modelling the degradation process of lithium-ion batteries when operating at erratic state-of-charge swing ranges," *2017 4th International Conference on Control, Decision and Information Technologies, CoDIT 2017*, pp. 860–865, 2017.

[25] Y. Cheng and Y. Tai, "A MILP Model for Optimizing Distributed Resource System with Energy Storage and PV Considering Energy Storage Life Loss," *2nd IEEE Conference on Energy Internet and Energy System Integration, EI2 2018 - Proceedings*, pp. 1–6, 2018.

[26] G. Cardoso, T. Brouhard, N. DeForest, D. Wang, M. Heleno, and L. Kotzur, "Battery aging in multi-energy microgrid design using mixed integer linear programming," *Applied Energy*, vol. 231, no. May, pp. 1059–1069, 2018.

[27] L. H. Macedo, J. F. Franco, R. Romero, and M. J. Rider, "An MILP model for the analysis of operation of energy storage devices in distribution systems," *2016 IEEE PES Transmission and Distribution Conference and Exposition-Latin America, PES T and D-LA 2016*, pp. 1–6, 2017.

[28] R. Guerrero and M. A. Pedrasa, "Component degradation and battery replacement in energy resource sizing for autonomous systems," *2018 IEEE Asia-Pacific Power and Energy Engineering Conference, APPEEC*, pp. 106–111, 2018.

[29] D. Fioriti, D. Poli, P. Cherubini, G. Lutzemberger, A. Micangeli, and P. Duenas-Martinez, "Comparison among deterministic methods to design rural mini-grids: Effect of operating strategies," *2019 IEEE Milan PowerTech, PowerTech 2019*, 2019.

[30] W. X. Shen, "Optimally sizing of solar array and battery in a standalone photovoltaic system in Malaysia," *Renewable Energy*, vol. 34, no. 1, pp. 348–352, 2009.

[31] C. Zhang, Y. Xu, and Z. Y. Dong, "Probability-weighted robust optimization for distributed generation planning in microgrids," *IEEE Transactions on Power Systems*, vol. 33, no. 6, pp. 7042–7051, 2018.

[32] G. G. Moshi, C. Bovo, A. Berizzi, and L. Taccari, "Optimization of integrated design and operation of microgrids under uncertainty," *19th Power Systems Computation Conference, PSCC 2016*, 2016.

[33] A. Vaccaro, M. Petrelli, and A. Berizzi, "Robust Optimization and Affine Arithmetic for Microgrid Scheduling under Uncertainty," *Proceedings - 2019 IEEE International Conference on Environment and Electrical Engineering and 2019 IEEE Industrial and Commercial Power Systems Europe, EEEIC/I and CPS Europe 2019*, pp. 1–6, 2019.

[34] IBM, "CPLEX User Manual," pp. 227–228, 2016.

[35] S. Pfenninger and I. Staffell, "Long-term patterns of European PV output using 30 years of validated hourly reanalysis and satellite data," *Energy*, vol. 114, pp. 1251–1265, 2016.

[36] I. Staffell and S. Pfenninger, "Using bias-corrected reanalysis to simulate current and future wind power output," *Energy*, vol. 114, pp. 1224–1239, 2016.

[37] E. Hartvigsson, M. Stadler, and G. Cardoso, "Rural electrification and capacity expansion with an integrated modeling approach," *Renewable Energy*, vol. 115, no. 2018, pp. 509–520, 2018.

[38] S. Mandelli, C. Brivio, E. Colombo, and M. Merlo, "A sizing methodology based on Levelized Cost of Supplied and Lost Energy for off-grid rural electrification systems," *Renewable Energy*, vol. 89, pp. 475–488, 2016.

[39] S. Ssewanyana and I. Kasirye, "Poverty and inequality dynamics in Uganda: Insights from the Uganda national Panel Surveys 2005/6 and 2009/10," *Research Series*, no. 94, 2012.

[40] X. Luo, J. Wang, M. Dooner, and J. Clarke, "Overview of current development in electrical energy storage technologies and the application potential in power system operation," *Applied Energy*, vol. 137, pp. 511–536, 2015.

[41] P. Haidl, A. Buchroithner, B. Schweighofer, M. Bader, and H. Wegleiter, "Lifetime analysis of energy storage systems for sustainable transportation," *Sustainability*, vol. 11, no. 23, 2019.

[42] M. Moncecchi, C. Brivio, S. Mandelli, and M. Merlo, "Battery energy storage systems in microgrids: Modeling and design criteria," *Energies*, vol. 13, no. 8, pp. 1–18, 2020.

[43] A. Malheiro, P. M. Castro, R. M. Lima, and A. Estanqueiro, "Integrated sizing and scheduling of wind/PV/diesel/battery isolated systems," *Renewable Energy*, vol. 83, pp. 646–657, 2015.